Title

Defect reduction in nonpolar a-plane GaN films using in situ SiNx nanomask

Journal

Applied Physics Letters, 89(4)

ISSN

0003-6951

Authors

Chakraborty, A
Kim, K C
Wu, F
et al.

Publication Date

2006-07-01

Peer reviewed

Defect reduction in nonpolar *a*-plane GaN films using *in situ* SiN_x nanomask

Arpan Chakraborty,[a] K. C. Kim, F. Wu, J. S. Speck, S. P. DenBaars, and U. K. Mishra
Electrical and Computer Engineering and Materials Departments, College of Engineering, University of California, Santa Barbara, California 93106

(Received 5 March 2006; accepted 3 June 2006; published online 25 July 2006)

We report on the use of *in-situ* SiN_x nanomask for defect reduction in nonpolar *a*-plane GaN films, grown by metal-organic chemical vapor deposition. High-resolution x-ray diffraction analysis revealed that there was a monotonic reduction in the full width at half maximum, both on-axis and off-axis, with the increase in the SiN_x thickness. Atomic force microscopy images revealed a significant decrease in the root-mean-square roughness and the density of submicron pits. Cross-section and plan-view transmission electron microscopy on the samples showed that the stacking fault density decreased from 8×10^5 to 3×10^5 cm^{-1} and threading dislocation density decreased from 8×10^{10} to 9×10^9 cm^{-2}. Room temperature photoluminescence measurement revealed that the band-edge emission intensity increased with the insertion of the SiN_x layer, which suggests reduction in the nonradiative recombination centers. © *2006 American Institute of Physics*. [DOI: 10.1063/1.2234841]

Recently, there has been considerable interest in the growth of nonpolar gallium nitride based epitaxial films, heterostructures, and devices.[1–5] Unlike conventional *c*-plane quantum wells, nonpolar (*a*- and *m*-plane) quantum wells are free of polarization-related electric fields along the growth direction.[6,7] However, heteroepitaxially grown planar *a*-plane GaN films are characterized by the presence of high dislocation density due to the large lattice mismatch with the available substrates.[2] The high defect density in planar films limits its device performance because threading dislocations act as nonradiative recombination centers and scattering centers and reduces radiative recombination efficiency, carrier mobility, and effect reliability. Therefore, improving the structural quality of nonpolar GaN films is pivotal to achieving high-performance devices. Lateral epitaxial overgrowth (LEO) techniques have been employed in the past for achieving defect reduction in nonpolar GaN.[8–10] However, all of these techniques involve *ex-situ* processing steps and regrowths. The use of *in-situ* SiN_x interlayer has proven to be an effective technique in defect reduction in conventional *c*-plane GaN.[11–13] In this letter, we report on the use of *in-situ* SiN_x nanomask for defect reduction in *a*-plane GaN films. The simplicity of an *in-situ* defect reduction growth method is highly attractive. Unlike traditional single-step LEO, the reduced feature size of the SiN_x nanopores facilitates nanometer-scale LEO, thereby resulting in defect reduction uniformly across the wafer.

The *a*-plane GaN films described herein were grown by metal-organic chemical vapor deposition, and the sample structure consisted of a low temperature GaN nucleation layer grown on *r*-plane sapphire substrate, followed by the growth of ~0.7 μm high temperature GaN. Trimethylgallium, ammonia (NH_3), and disilane (Si_2H_6) were used as Ga, N, and Si sources, respectively. Then a thin layer of SiN_x was inserted by flowing disilane and ammonia. The thickness of the SiN_x interlayer was controlled by varying the growth time. The SiN_x layer was followed by the growth of a ~0.1 μm thick unintentionally doped GaN layer and capped with a ~2 μm thick Si-doped GaN layer. The Si concentration ($[Si]\sim7\times10^{18}$ cm^{-3}) in the Si-doped GaN layer was much higher than the compensation level ($\sim1\times10^{18}$ cm^{-3}) (Ref. 14). Secondary-ion-mass-spectroscopy (SIMS) measurement revealed that the Si-doping profile in the Si-doped GaN layer was not affected by the thickness of the SiN_x layer. After the growth, the surface morphology of the as-grown samples was studied by means of Nomarski-mode optical microscopy and atomic force microscopy (AFM). A Digital Instruments D3000 AFM was used in the tapping mode to image the surface of the samples. The crystalline quality and the crystal mosaic of the as-grown films were determined using a Philips four-circle MRD x-ray diffractometer using Cu $K\alpha$ radiation operating in receiving slit mode with a four bounce Ge (220) monochromator and a 1.2 mm slit on the detector arm. Transmission electron microscopy (TEM) was used to correlate the x-ray measurements to the microstructure of *a*-plane GaN grown with and without SiN_x interlayer. $[1\bar{1}00]$ cross-section and plan-view samples were prepared with a FEI focused ion beam instrument (model DB235 dual beam). Two beam diffraction contrast bright field and dark field images were recorded using an FEI Tecnai G2 Sphera Microscope, operated at 200 kV. Room temperature photoluminescence (PL) measurements were carried out using the 325 nm line of a cw He–Cd laser with an excitation power density of ~20 W/cm^2.

The Nomarski image of a fully coalesced *a*-plane GaN film with 120 s of SiN_x interlayer revealed smooth and uniform surface with a few occasional pits formed from the coalescence edge. 5×5 μm^2 AFM images of samples with and without SiN_x nanomask are shown in Fig. 1(a) and 1(b), respectively. There was a significant improvement in the surface morphology after the insertion of SiN_x interlayer. There was a reduction in the density of submicron pits, and the rms roughness decreased from 2.6 to 0.6 nm.

Omega x-ray rocking curves (XRCs) were measured for both the GaN on-axis (110) and off-axis (100), (101), (201), and (102) reflections. The on-axis and off-axis XRCs of

[a]Electronic mail: arpan@ece.ucsb.edu

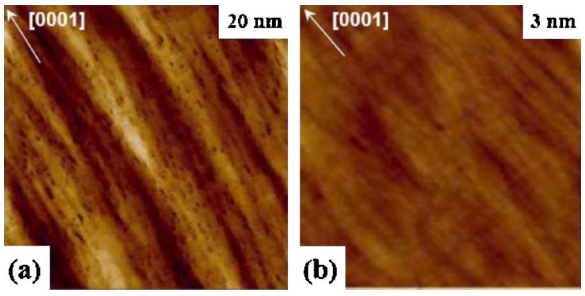

FIG. 1. (Color online) 5×5 μm^2 AFM micrographs of 2 μm thick *a*-plane GaN template (a) without SiN_x interlayer and (b) with 120 s of SiN_x interlayer.

samples grown with different SiN_x growth time were measured and the full width at half maximum (FWHM) of the measurements are plotted in Fig. 2. The on-axis FWHMs of $\phi=0°$ and $\phi=90°$ (*c*- and *m*-mosaics, respectively) for GaN template without SiN_x interlayer were 0.69° (1290″) and 0.36° (2471″), respectively. The (101) off-axis peak, which measures the "twist" mosaic, had a FWHM of 0.64° (2292″). These large FWHM values are in agreement with the high dislocation density typically observed in planar *a*-plane GaN.[2] It can be seen that the on-axis and off-axis FWHM for

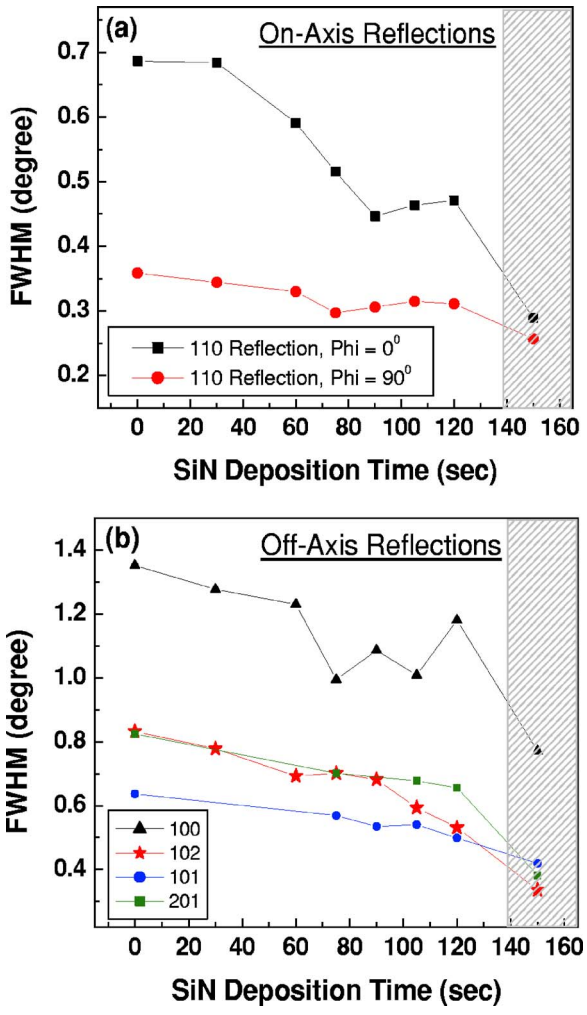

FIG. 2. (Color online) (a) On-axis and (b) off-axis XRC FWHMs of *a*-plane GaN templates with different SiN_x deposition times. The shaded region shows the sample which remained uncoalesced after 2 μm of GaN overgrowth.

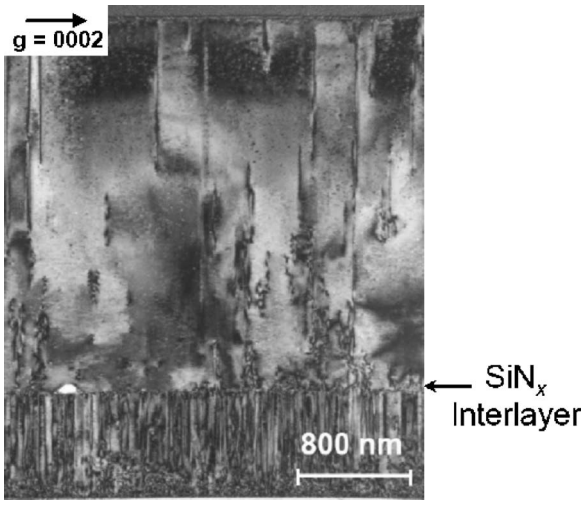

FIG. 3. Cross-section TEM image of *a*-plane GaN template with 150 s of SiN_x interlayer. The diffraction condition is $\mathbf{g}=0002$.

all of the reflections decreased with the increase in the SiN_x deposition time. This decrease signified dislocation reduction with the SiN_x nanomasking.[15,16] It was also noted that for the on-axis scan, the ratio of *m* mosaic to *c* mosaic approached unity with the increase in the SiN_x growth time. The minimum XRC FWHMs were obtained for 150 s of SiN_x deposition, and the on-axis values were 0.29° (1040″) and 0.25° (924″) for $\phi=0°$ and $\phi=90°$, respectively. The off-axis values were 0.42° (1508″), 0.38° (1375″), and 0.33° (1208″) for (101), (201), and (102) reflections, respectively. However, the sample grown with 150 s of SiN_x growth could not be coalesced completely after 2 μm of GaN overgrowth.

TEM was performed on samples with SiN_x growth time of 0, 120, and 150 s. The cross-section image of the sample with 150 s of SiN_x interlayer is shown in Fig. 3. From the cross-section image, it was observed that the threading dislocations (TDs) have a common line direction, parallel to the $[11\bar{2}0]$ growth direction, for all the samples. Significant blocking of the extended defects was observed at the GaN–SiN_x interface. Thus it was evident that dislocation reduction was indeed achieved by the insertion of the SiN_x interlayer. In addition to the TDs, plan-view TEM on the samples revealed stacking faults (SFs) aligned perpendicular to the *c*-axis. The TD and the SF density for the samples were determined from the plan-view images, and the values are summarized in Table I. It is evident from the table that both TD and SF density decreased as a result of the SiN_x nanomasking, which concurs with the XRC findings.

The room temperature PL intensity of the GaN band-edge improved with the SiN_x nanomasking (shown in Fig. 4). The *a*-GaN sample without the SiN_x interlayer did not show band-edge emission. However, with the increase in the SiN_x thickness, PL emission intensity increased. Also, PL emission from AlGaN/GaN multiple-quantum wells, grown on the samples with different SiN_x thicknesses, showed a simi-

TABLE I. Summary of the TEM results.

SiN_x deposition time (s)	0	120	150
TD Density (cm^{-2})	$6\times10^{10}-8\times10^{10}$	$1\times10^{10}-3\times10^{10}$	9×10^{9}
SF density (cm^{-1})	$6\times10^{5}-8\times10^{5}$	4×10^{5}	3×10^{5}

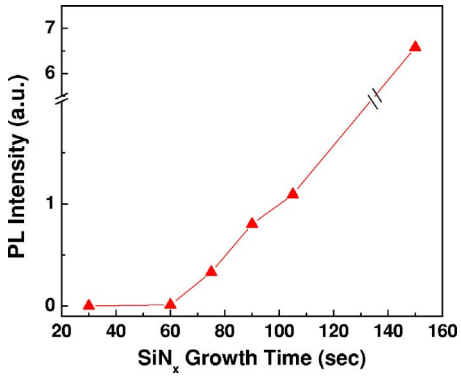

FIG. 4. (Color online) Improvement of the GaN band-edge PL emission with the increase in SiN_x growth time.

lar trend. The increased emission intensity is probably a consequence of reduction in the TD density. The much increased emission intensity from the sample with 150 s of SiN_x is probably due to the increased light extraction from the uncoalesced facets of the sample.

In conclusion, we have demonstrated the effectiveness of *in-situ* SiN_x nanomask in defect reduction in *a*-plane GaN films grown on *r*-plane sapphire. The thickness of SiN_x interlayer was varied by changing the growth time. The use of SiN_x resulted in the reduction of on-axis and off-axis XRC FWHMs and also resulted in the reduction of rms roughness in AFM images. Cross-section and plan-view TEM micrographs revealed reduction in defect density—both SFs and TDs. The intensity of band-edge luminescence improved due to the reduction in defect density.

The authors would like to acknowledge the support of SSLDC, JST/ERATO, and the National Science Foundation for use of facilities through the MRSEC program.

[1]P. Waltereit, O. Brandt, A. Trampert, H. T. Grahn, J. Menniger, M. Ramsteiner, M. Reiche, and K. H. Ploog, Nature (London) **406**, 865 (2000).
[2]M. D. Craven, S. H. Lim, F. Wu, J. S. Speck, and S. P. DenBaars, Appl. Phys. Lett. **81**, 469 (2002).
[3]H. M. Ng, Appl. Phys. Lett. **80**, 4369 (2002).
[4]Y. J. Sun, O. Brandt, S. Cronenberg, S. Dhar, H. T. Grahn, K. H. Ploog, P. Waltereit, and J. S. Speck, Phys. Rev. B **67**, 041306 (2003).
[5]A. Chakraborty, B. A. Haskell, S. Keller, J. S. Speck, S. P. DenBaars, S. Nakamura, and U. K. Mishra, Appl. Phys. Lett. **85**, 5143 (2004).
[6]S. F. Chichibu, T. Sota, and S. Nakamura, Appl. Phys. Lett. **69**, 4188 (1996).
[7]F. Bernardini, V. Fiorentini, and D. Vanderbilt, Phys. Rev. B **56**, R10024 (1997).
[8]M. D. Craven, S. H. Lim, F. Wu, J. S. Speck, and S. P. DenBaars, Appl. Phys. Lett. **81**, 1201 (2002).
[9]C. Chen, J. Zhang, J. Yang, V. Adivarahan, S. Rai, S. Wu, H. Wang, W. Sun, M. Su, Z. Gong, E. Kuokstis, M. Gaevski, and M. A. Khan, Jpn. J. Appl. Phys., Part 2 **42**, L818 (2003).
[10]B. Imer, F. Wu, S. P. DenBaars, and J. S. Speck, Appl. Phys. Lett. **88**, 061908 (2006).
[11]S. Sakai, T. Wang, Y. Morishima, and Y. Naoi, J. Cryst. Growth **221**, 334 (2000).
[12]S. Tanaka, M. Takeuchi, and Y. Aoyagi, Jpn. J. Appl. Phys., Part 2 **38**, L831 (2000).
[13]F. Yun, Y.-T. Moon, Y. Fu, K. Zhu, Ü. Ozgür, H. Morkoç, C. K. Inoki, T. S. Kuan, A. Sagar, and R. M. Feenstra, J. Appl. Phys. **98**, 123502 (2005).
[14]M. D. Craven, A. Chakraborty, B. Imer, F. Wu, S. Keller, U. K. Mishra, J. S. Speck, and S. P. DenBaars, Phys. Status Solidi C **0**, 2132 (2003).
[15]B. Heying, X. H. Wu, S. Keller, Y. Li, D. Kapolnek, B. P. Keller, S. P. DenBaars, and J. S. Speck, Appl. Phys. Lett. **68**, 643 (1996).
[16]V. Srikant, J. S. Speck, and D. R. Clarke, J. Appl. Phys. **82**, 4286 (1997).